African Journal of Educational Studies in Mathematics and Sciences Vol. 9, 2011

Effect of duct orientation on particle deposition in the human respiratory tract

Asiedu-Addo[1], S. K. & Bentil[2], D. E.

Abstract

A two-dimensional model of transport and deposition of particles in the human acinus is formulated. The model simulates airway generations 20-23 of the respiratory tract by solving numerically the system of Navier-Stokes equations for continuity and momentum. The finite volume method under the platform of the FLUENT code was employed to perform the numerical calculations and the fully implicit discretization approach was used for discretizing the transient equations on the grounds of its superior stability. The simulations of macron size particles (1-5 μm) show that the existence of alveolar re-circulation and gravity orientation are key factors in determining the deposition in the last four generations of the human respiratory tract.

Keyword duct orientation, particle deposition, respiratory tract, discretization approach

Introduction

Over the years, a number of studies, both experimentally and theoretically, have been devoted to the mathematical modeling of gas transport in the human respiratory tract (see for example, Paiva and Demeester, (1971), Chang and Farhi, (1973); Paiva, (1973), Stibitz, 1973), Tsuda et al., (1994), Darquenn and Paiva (1996) and Darquenne (2001). The motivation for such studies is due to the fact that, modeling the deposition of particles in the respiratory tract presents practical scientific tools worthy of being actively employed in the field of medicine which is essential in contemporary science and mathematics. Mathematical modeling of aerosol particles in the respiratory tract does not only help interpret experimental data, but also allow predictions to be made for cases where experimental data are not available as it is the case in the alveolar region of the lung. It may also explain the origin of pulmonary diseases induced by respirable microorganisms such as bacteria, fungi and viruses.

Different processes, acting simultaneously in the human respiratory tract determine the transport and fate of inhaled aerosol particles. These processes are inertial impaction, gravitational sedimentation and Brownian diffusion. The contributions of these processes to particle transport and deposition in local airway segments vary with effective particle size, density, local airflow rate and gravity angle (Kleinstreuer et al., 2007). Inertial impaction mechanism dominates the large airways and several earlier researchers had concentrated on modeling the first few airway generations, using the bend tube to study inertial deposition of particles in the airways (see for example Landahl (1950), Diu and Yu (1980), Cheng and Wang (1981)). Gravitational sedimentation and Brownian

1 Asiedu-Addo * S. K. is a Senior Lecturer at the Department of mathematics, University of Education, Winneba, Ghana.

2 Bentil, D. E. is a Mathematics Professor, at the Department of Mathematics and Statistics, University of Vermont, Burlington, USA

diffusion are important in small airways which have been well formulated since flow conditions in those airways are relatively simple (Ingman, 1975, Pich, 1972, Yu and Thiagarajan, 1978).

In this study, we developed a two dimensional gravitational deposition model in the 20-23 generations of the alveolar region of the acinus. The motivation for this study is due to the fact that, direct experimental studies of gravitational deposition in human respiratory system are hardly available. Published data only include regional deposition fractions in the alveolar region where sedimentation may be dominant or occurs in conjunction with diffusion and impaction (Kleinstreuer et al., 2007). Traditionally, gravitational deposition in the tracheobronchial airways and the alveolar ducts is estimated via analytical equations derived from the sedimentation losses in flows between parallel plates or in circular tubes (see for example Asgharian, et al., 2006; Beeckmans, 1965; Pich, 1972).

From the point of view of Moskal and Gradon, (2002), mathematical modeling of any particle deposition in the respiratory tract should consist of the following elements: the deposition mechanisms of the aerosol particles with the given physiochemical properties, morphology and the geometry of the respiratory system and the fluid dynamics of the respiratory airflow (mathematical formulation).

Morphology and the geometry of the respiratory system

The morphology of the human lung incorporated in our model is based on experimental data of Weibel Model "A" (1963). This model has provided a good basis for the development of a range of increasing sophisticated gas transport and mixing models and it is the most commonly used conducting airway model. (Tawhai et al., 2000)

Many models of airway structure and geometry have been proposed due to the complex nature of the human reparatory tract which has some common geometric characteristics (see for example Weibel (1963), Horsfeld and Cumming (1967)). In this study, a two-dimensional geometric structure representing the 20-23 generations of the alveolar region of the acinus was considered. Geometrically, we employed Weibel's model "A" (1963) and considered the lung as a hollow cylinder that leads to the acinus (see Figure 1). The acinus is therefore considered as a compact bounded structure with one inlet from which the carrier gas enters the structure.

In general, gravitational sedimentation is important for micron particles (1-10 μm) in the lower airways and alveolar regions, where the Reynolds numbers are low (Kleinstreuer et al., 2007). Because these particles are too large to undergo significant thermal diffusion and too light to be substantially affected by inertia, their fate may predominantly be determined by the balance between aerodynamic and gravitational forces Heyder et al., (1985).

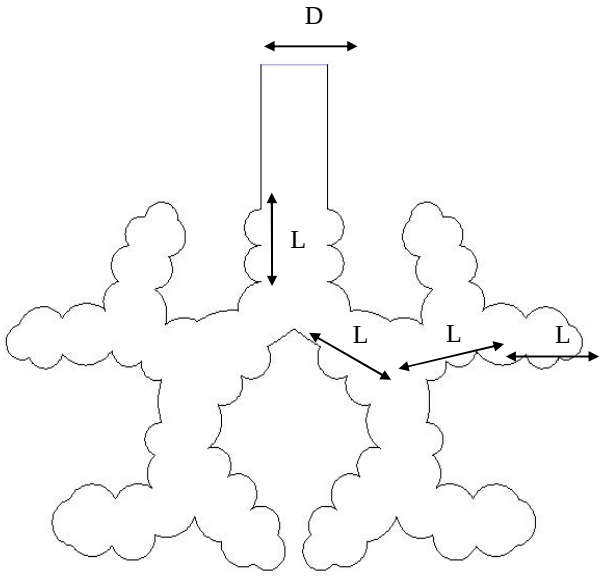

Figure 1 Two-dimensional geometric structure representing the 20-23 generations of the alveolar region of the acinus's

Mathematical formulation

The governing mathematical equations of this study are described by the system of the Navier-Stokes equations consisting of conservation of mass and momentum equations. The Navier-Stokes equations are based on the assumptions that the fluid, at the scale of interest, is a continuum and that all the of fields of interest like pressure, velocity, density, temperature and so on, are differentiable, weakly at least.

Regardless of the flow assumptions, a statement of the conservation of mass is nearly always necessary. This is achieved through the mass continuity equation, given in its most general form as:

$$\frac{\partial \rho}{\partial t} + \nabla \cdot (\rho \mathbf{v}) = 0 \qquad (1)$$

The vast majority of work on the Navier-Stokes equations is done under an incompressible flow assumption for Newtonian fluids. Taking the incompressible flow assumption into account and assuming constant viscosity, the Navier-Stokes equations will read (in vector form):

$$\overbrace{\rho(\underbrace{\frac{\partial \mathbf{v}}{\partial t}}_{\substack{\text{Unsteady}\\ \text{acceleration}}} + \underbrace{\mathbf{v} \cdot \nabla \mathbf{v})}_{\substack{\text{Convective}\\ \text{acceleration}}}}^{\text{Inertia}} = \underbrace{-\nabla p}_{\substack{\text{Pressure}\\ \text{gradient}}} + \underbrace{\mu \nabla^2 \mathbf{v}}_{\text{Viscosity}} + \underbrace{\mathbf{f}}_{\substack{\text{Other}\\ \text{forces}}} \qquad (2)$$

where, $\mathbf{v}$ is the fluid phase velocity, μ is the molecular viscosity of the fluid, ρ is the fluid density, and f represents "other" body forces (forces per unit volume), such as gravity. In equation (2), only the convective term is nonlinear for incompressible

Newtonian flow.

The airflow in the airway model 20-23 generations is assumed to be steady, incompressible and laminar. The set of unsteady conservation equations governing the air velocity fields is given by the Navier–Stokes equations consisting of conservation of mass, equation (1), and momentum, equation (3).

$$\frac{\partial(\rho \mathbf{v})}{\partial t} + \nabla \cdot (\rho \mathbf{v}\mathbf{v}) = -\nabla \mathrm{p} + \mu \nabla^2 \mathbf{v} + \rho \mathbf{g} \qquad (3)$$

where, $\mathbf{v}$ is the fluid phase velocity, μ is the molecular viscosity of the fluid, ρ is the fluid density, and $\mathbf{g}$ is the gravitational acceleration. The boundary conditions employed in this work is the No-Slip boundary conditions which requires that the fluid in contact with a continuous walls be at rest. That is

$$u \times \hat{n} = U \times \hat{n},$$

where, u is the fluid velocity, U is the velocity of the wall and $\hat{n}$ is a unit vector. In fluid dynamics, the No-Slip boundary conditions for viscous fluid states that at a solid boundary, the fluid will have zero velocity relative to the boundary. The trajectory of the particles is predicted by integrating the force balance on the particle. This force balance equates the particle inertia with the forces acting on the particle and can be written as

$$\frac{d\mathbf{v}_p}{dt} = F_D(\mathbf{v} - \mathbf{v}_p) + \frac{\mathbf{g}(\rho_p - \rho)}{\rho_p}, \qquad (4)$$

where $\mathbf{v}_p$ is the particle velocity, $\mathbf{v}$ is the fluid phase velocity, ρ is the fluid density, ρ_p, the particle density, $\mathbf{g}$, gravitational acceleration coefficient. The drag force, $F_D(\mathbf{v} - \mathbf{v}_p)$ is calculated from the expression

$$F_{\mathrm{D}} = \frac{18\mu}{\rho_{\mathrm{p}} \mathrm{d}_{\mathrm{p}}^2} \frac{\mathrm{C}_{\mathrm{D}} \mathrm{Re}_{\mathrm{p}}}{24}. \qquad (5)$$

Here, μ is the molecular viscosity of the fluid, d_{p} is the particle diameter and Rep is the relative Reynolds number, which is defined as

$$\mathrm{Re}_{\mathrm{p}} \equiv \frac{\rho \mathrm{d}_{\mathrm{p}} \left| \mathbf{v}_{\mathrm{p}} - \mathbf{v} \right|}{\mu}. \qquad (6)$$

At small Reynolds number (Re ~ 0.1), which is the case of this study, the flow is known as Stokes flow and under these conditions the drag force coefficient C_{D} is given by

$$\mathrm{C}_{\mathrm{D}} = \frac{24}{\mathrm{Re}_{\mathrm{P}}}. \qquad (7)$$

The magnitude of the Reynolds number, Re, may be regarded as providing an estimate of the relative importance of the non-viscous and viscous forces acting on unit volume of

the fluid.

Numerical Computations

The velocity field of the carrier gas is computed in the 2D alveolated ducts by solving Navier-Stokes equations (1) and (3) with existing software based on a finite volume procedure (FLUENT). This procedure involves the subdivision of the domain into a finite number of control volumes or cells over which the differential equations are discretized using the fully implicit discretization method. Because of the nonlinearity and the interdependence of these equations, an iterative solution procedure is adopted. Since the flow is incompressible and the structure is rigid, it is as if the volume variations take place at the end of the alveolar ducts of the last generation.

During the simulation process, the properties of air were taken as constants and are evaluated at a temperature of 37˚C except density which vary following the ideal gas equation. The simulations which started from the mouth had inlet velocity fixed at v_i = 0.003 m/s are based on 2s inspiration with a fixed time step of 0.01s and 20 iterations per time step. At the beginning of each time step, 30 particles (made out of wood) are injected uniformly at the inlet from t = 0 for 1s period. A particle is considered deposited when it touches the surface for the first time.

The basic premise of the present model is that alveolar flow can be considered as creeping (inertialess) flow. This assumption is justifiable, at least as a first-order approximation, because the Reynolds number of airflow in the acinus is generally much smaller than unity.

Inasmuch as the particle size plays a major role in particle dynamics, simulations were done for different particle diameters. In this work, micron-sized particles $(1 < d_p < 5\ \mu m)$ were considered for simulation for different positions of the geometric model with respect to the gravitational field. The different positions of the model are given by the angle between the axis of the duct of the first generation and the horizontal plane. Four positions were considered: $\vec{g}$ [-g, 0], (b) $\vec{g}$ [0, -g], (c) $\vec{g}$ [-0.71g, -0.71g], and (d) $\vec{g}$ [-0.71g, 0.71g] in this work. Once the particle positions are accurately obtained at the end of each time step, we proceed to calculate the average particle concentration from the relation

$$C = \frac{M_s}{V} \qquad (8)$$

where Ms is the total mass of suspended particles (mg), and V is the total volume of the structure (mm3).

Analysis and Discussion

Figure 1 (a-d) show the effect of gravity orientation on aerosol distribution of 1 µm particle diameter in the ascinus. The gravity orientations used in the simulation are: (a) $\vec{g}$ [-g, 0], (b) $\vec{g}$ [0, -g], (c) $\vec{g}$ [-0.71g, -0.71g], and (d) $\vec{g}$ [-0.71g, 0.71g].

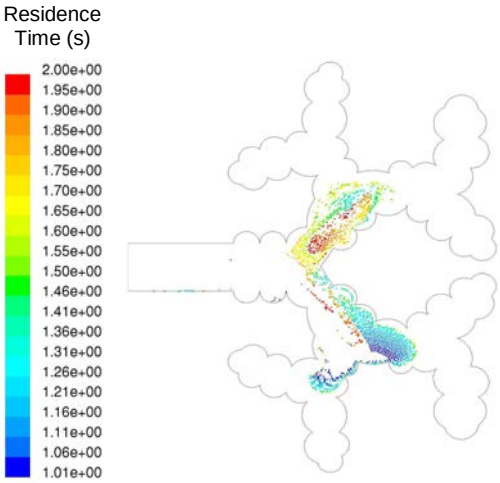

Figure 1 (a). Effect of gravity orientation on aerosol distribution of 1 µm particle diameter: $\vec{g}$ [-g,0]

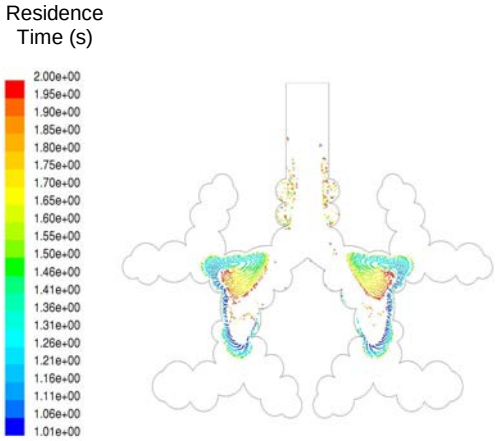

Figure 1 (b). Effect of gravity orientation on aerosol distribution of 1 µm particle diameter: $\vec{g}$ [0,-g]

The colors differentiate the particles by their residence time in seconds after injection. For this small particle size the effect of the gravity on the particle distribution is limited. This is clear in Figure. 1 (a) where a significant number of particles are flowing into the right side of the geometry that is opposite to the gravity direction. This observation is confirmed by Kleinstreuer et al., (2007). They showed that particles essentially settle on the walls of the respiratory tract which is normal to the gravity direction.

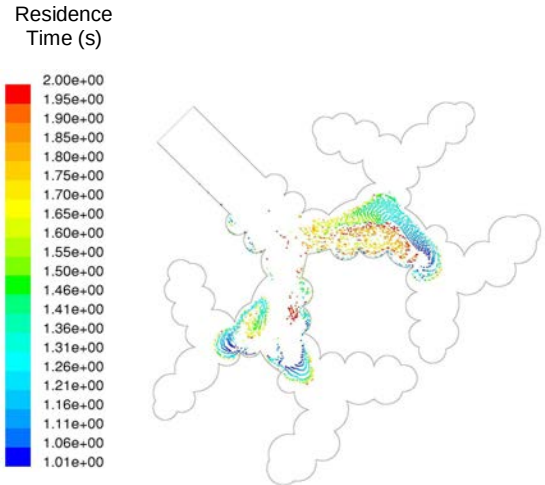

Figure 1 (c). Effect of gravity orientation on aerosol distribution of 1 µm particle diameter: $\vec{g}$ [-0.71g, -0.71g]

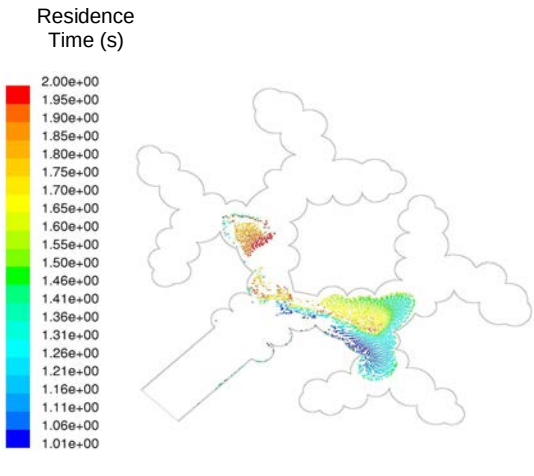

Figure 1 (d). Effect of gravity orientation on aerosol distribution of 1 µm particle diameter: $\vec{g}$ [-0.71g, 0.71g]

In Figure 2 (a-d), particle diameter of 5 µm was also simulated and the effects of gravity of different orientation on aerosol were observed. The colors differentiate the particles by their residence time in seconds after injection. The gravity orientations were:

(a) $\vec{g}$ [-g, 0], (b) $\vec{g}$ [0, -g], (c) $\vec{g}$ [-0.71g, -0.71g], and (d) $\vec{g}$ [-0.71g, 0.71g].

We observe that gravity plays a vital role in determining the trajectories of large particles and that 5 µm particles deposit deeper within the acinus and the orientation of gravity has an influence on their deposition patterns.

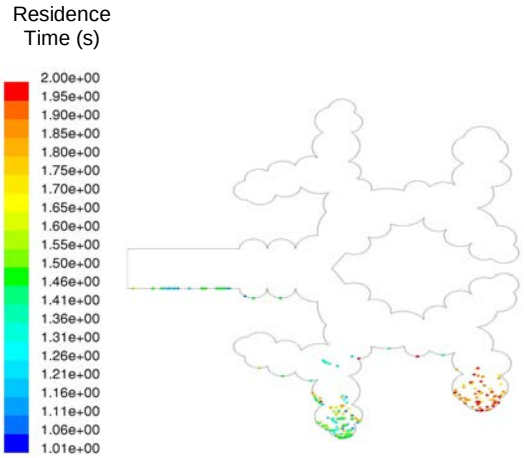

Figure 2 (a). Effect of gravity orientation on aerosol distribution of 5 µm particle diameter: $\vec{g}$ [-g, 0]

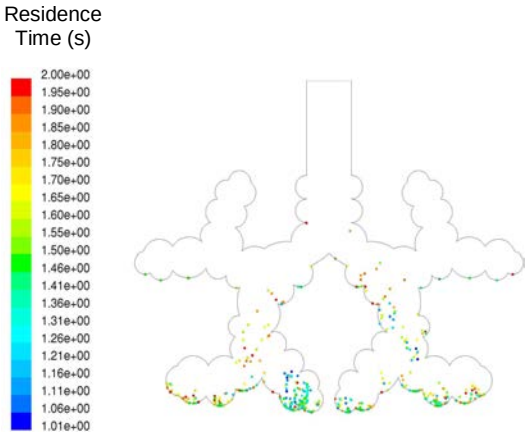

Figure 2 (b). Effect of gravity orientation on aerosol distribution of 5 µm particle diameter: $\vec{g}$ [0,-g]

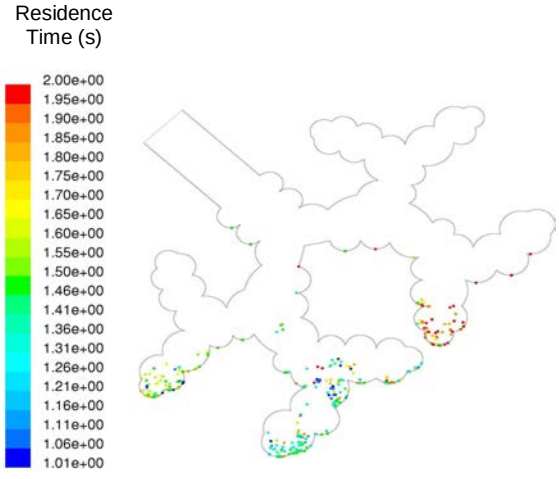

Figure 2 (c). Effect of gravity orientation on aerosol distribution of 5 µm particle diameter: $\vec{g}$ [-0.71g, -0.71g]

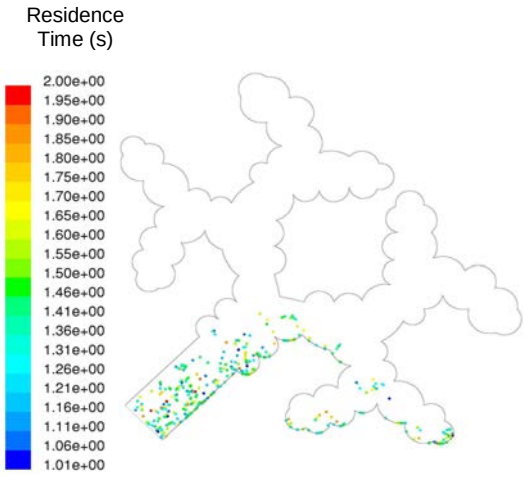

Figure 2 (d). Effect of gravity orientation on aerosol distribution of 5 µm particle diameter: $\vec{g}$ [-0.71g, 0.71g]

The effect of gravity orientation on particle deposition for various particle sizes is presented in Figure 3. In this figure, the aerosol percentage deposition in the 2D structure is plotted as a function of gravity orientation for the three particle size. We see from the graph that total deposition increases monotonically with the particle size. For 1 µm and 3 µm particles, the total deposition is slightly affected by the gravity.

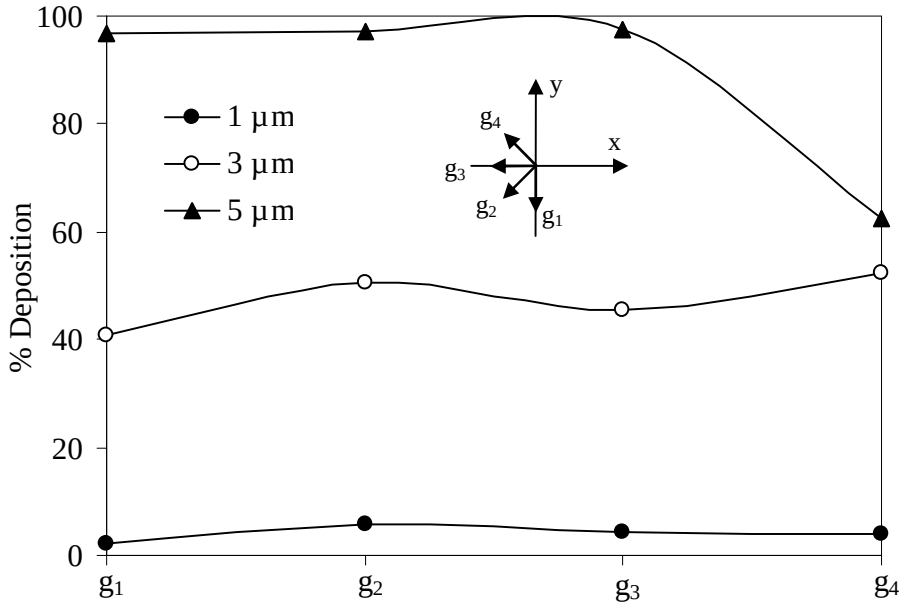

Figure 3 Effect of gravity orientation on particle deposition for particles of sizes 1 µm, 3 µm and 5 µm.

However, the deposition of 5 µm particles decreases significantly when the gravity is orientation is in g_4 direction. This is due to the fact that, in this position, the particles that remain in suspension at the end of the inspiration phase are located near the entrance of the ducts of the 20^{th} generation which is positioned vertically. In this generation, the velocity of the carrier gas is several times smaller than the settling velocity, and particles cannot go upstream. During the expiration, those particles travel in the middle of the central ducts without reaching any alveolar wall and are then expired at the end of the simulated breadth. For 5 µm diameter particles, the deposition sites inside the alveoli depend greatly on the duct orientation, and large non-uniformities appear in the pattern of deposited particles. This is emphasized in Figure 3 where, deposition of particles increase gently and reached a maximum at g_3 before they decrease smoothly in g_4. This is due to the coupled effect of curved streamlines near the entrance of the alveoli and gravity, which directs the particles against the bulk flow. It results in a force turned toward the alveolar cavities.

In Figure 4, simulation of deposition as a percentage of particles injected at the inlet is shown. The results indicate deposition of particles versus particle diameter for four gravity orientations. In addition to the increment of deposition with the particle weight, the orientations g_1, g_2, and g_3 present similar trend with a maximum difference of about

10% at d = 3 µm. The g_4 orientation provides higher deposition for small particles with d $\leq$ 3 µm and lower deposition for large particles with d $\geq$ 3 µm.

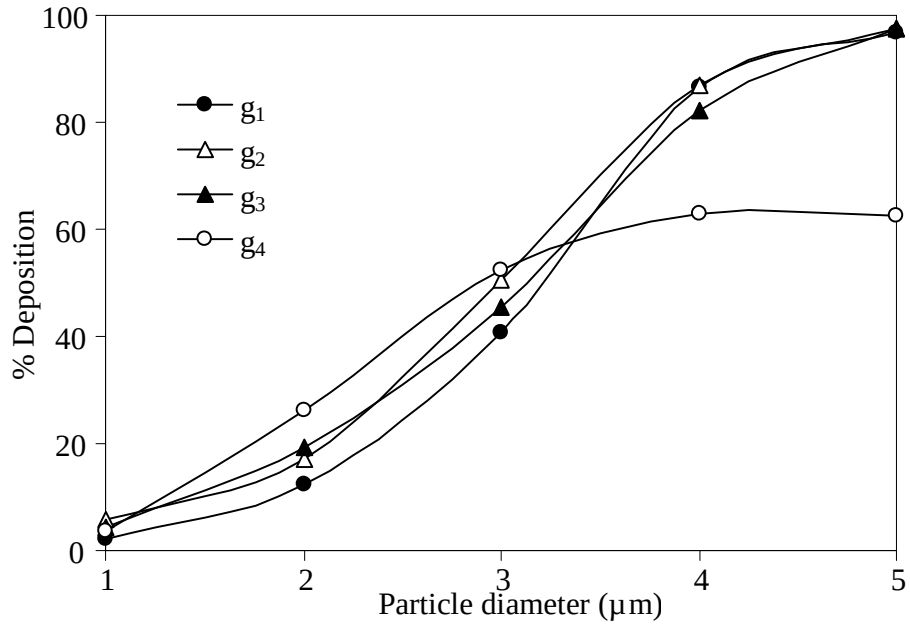

Figure 4 Deposition, as a percentage of particles injected at the inlet, versus particle diameter for four gravity orientations.

Figure 4 demonstrates that the presence of gravity may increase particle deposition in the acinus region, as the particle size increases. Figure 5 shows the variations of the total particle concentration with time for various particle sizes. Since the particles are injected during the first second, the concentration increases with time in the interval [0, 1s] for all particle sizes. In the interval [1s, 2s] the concentration decreases due to the deposition and the concentration of larger particles decreases quickly. This is due to the fact that larger particles reach terminal velocities faster than smaller particles and therefore have shorter residence time

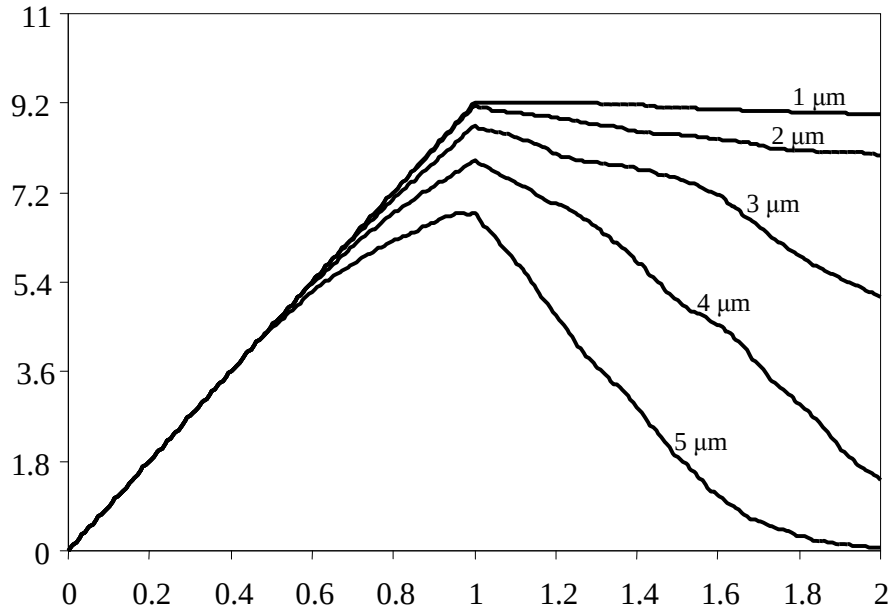

Figure 5 Variations of the total particle concentration with time forvarious particle sizes.

This process therefore ensures that particles with larger diameter are deposited on the walls of the alveolar region. It is also clear from Figure 5 that the maximum of the concentration curve is disproportional to the particle size. This confirms the work of Haber et al. (2003) that in the alveolus, the concentration of larger particles decreases quickly and thus enhances deposition.

Conclusion

The objective of this study was to investigate the influence of the flow field induced by gravity orientation and particle size deposition in the human acinus by using two-dimensional simulations of a branching structure representative of an acinus. The simulations were done for generations 20-23.

The results suggest that: (1) the flow pattern computed in the inlet indicates that the flow enters the alveoli and re-circulates slowly inside them. Inside the alveoli the velocity of the carrier gas is quite negligible, and particles move only under the action of gravity and the deposition sites inside the alveoli depend greatly on the duct orientation (Figure 1); (2) the velocity magnitudes are larger than the average flow velocity in the 20^{th} and the 21^{st} generations and gravity orientation has effects on aerosol deposition within the acinus. For example in Figure 1 (a), a significant number of particles are flowing into the right side of the geometry which is opposite to the gravity direction; (3) for the particles that we considered in this simulations (1-5 μm), during the early stages of inspiration, the velocity of ductal airflow is still small, and the particles move appreciably downward due to gravity, entering the alveolus.

Once the particles are inside the alveolus, they tend to follow the alveolar re-circulation flow due to their gravity orientation. But due to their heavy weight, these particles continue to settle downward and soon are deposited. This is evidenced in Figure 4 where

the graph shows that there is increment of deposition with increase in particle weight and they are affected by gravity orientation. The new model reported here demonstrates that the existence of alveolar re-circulation and gravity orientation are key factors in determining the gravitational deposition in the last four generations of the human respiratory tract.

References

Asgharian, B., Price, O. and Oberdorster, G. (2006). A modeling study of the effect of gravity on airflow distribution and particle deposition in the lung. *Inhalation Toxicology*, **18**, pp 473-481.

Beeckmans, J. M. (1965). The deposition of aerosols in the respiratory tract 1. Mathematical anaysis and comparison with experimental data. *Canadian Journal of Pharmacology*. **43**, pp 157-172.

Chang, H. K. and Farhi, L. E. (1973). On mathematical analysis of a gas transport in the lung. *Respir. Physiol*. **18,** pp 370-385.

Cheng, Y. S. and Wang, C. S. (1981). Motion of particles of Circular Pipes. Atmospheric Environment, Vol 15, pp301-306.

Darquenne, C. (2001). A realistic two-dimensional model of aerosol transport and deposition in the alveolar zone of the human lung. *J. of Aerosol Sci*. **32:** pp 1161-1174.

Darquenne, C. and Paiva, M. (1996). Two- and three-dimensional simulations of aerosol transport and deposition in alveolar zone of human lung. *J. of Appl. Physiol.* **80 (4),** pp 1401-1414.

Diu, C. K. and Yu, C. P. (1980). Deposition from charged Aerosol flows through a Two-Dimensional Bend, J. of Aerosol Science, Vol11, pp391-395

Haber, S., Yitzhak, D. and Tsuda, A. (2003). A. Gravitational deposition in a rhythmically expanding and contracting alveolus. *J. Appl. Physiol,* **95**, pp 657-671.

Heyder J., Gebhart, J. and Scheuch, G. (1985). Interaction of diffusional gravitational particle transport in aerosols. *Aerosol Science Technology* **4**, pp 315-326.

Horsfield, K. and Cumming, G. (1967). Morphology of the bronchial tree in man, *J. Appl. Physiol.* **24**, 373-383.

Ingman, D. B. (1975). Diffusion of Aerosols from Stream Flowing through a Cylindrical Tube. *Journal of Aerosol Science* Vol. **6** pp 125-132.

Kleinstreuer, C., Zhang, Z., and Kim, C.S., (2007). Combined inertial and gravitational deposition of microparticles in small model airways of a human respiratory system, *J. aerosol Science*, **38**, pp 1047-1061.

Landahl, H. D. (1950). On the removal of airborne droplets by the human respiratory tract I, The Lung. *Bulletin of Mathematics and Physics,* **12:** 43-56.

Moskal, A. and Gradon, L. (2002). Temporary and spatial deposition of Aerosol particles in the upper human airways during breathing cycle, *J. aerosol Science*, **33**, pp 1525-1539.

Paiva, M. (1973). Gas transport in the human lung. *J. Appl. Physiol*. **35**, pp 401-410.

Paiva, M. and Demeester, M. (1971). Gas transport in the air phase of the lung simulated by a digital computer. *Comp. Biomed. Res*. **3**, pp 675-689.

Pich, J. (1972). Theory of gravitational deposition of particles from laminar flows in channels. *J. Aerosol Science*, **3**, pp 351-361.

Sapoval, B. Filoche M. and Weibel, E. R. (2002). Smaller is better-but not too small: A physical scale for the design of the mammalian pulmonary acinus. *PNAS.* **99:** 10411-10416.

Stibitz, G. R. (1973). A model of diffusion in respiratory unit. *Respir. Physiol*. **18**, pp 249-257.

Tawhai, M. H., Pullan, A. J. and Hunter, P. J. (2000). Generation of an Anatomically Based Three-Dimensional Model of the Conducting Airways. *Annals of Biomedical Engineering*, **28**, 793-802.

Tsuda, A., Butler, J. P., and Fredberg, J. J. (1994). Effects of alveolated duct structure on aerosol deposition in the pulmonary acinus II: Gravitational Sedimentation and initial impaction in the absence of diffusion. *J. Appl. Physiol.,* **76:** pp 2510-2516.

Weibel, E. R. (1963). *Morphometry of Human Lungs*. Berlin: Springer-Verlag.

Yu C. P. and Thiagarajan, V. (1978). Sedimentation of Aerosols in closed finite tubes in random orientation. *J. Aerosol Science*, Vol **9**, 315-320.